

# 3D Numerical Analysis of an ACL Reconstructed Knee

M. Chizari, B. Wang

School of Engineering, University of Aberdeen, Aberdeen AB24 7QW, UK

*Abstract: Numerical methods applicable to the tibia bone and soft tissue biomechanics of an ACL reconstructed knee are presented in this paper. The aim is to achieve a better understanding of the mechanics of an ACL reconstructed knee. The paper describes the methodology applied in the development of an anatomically detailed three-dimensional ACL reconstructed knee model for finite element analysis from medical image data obtained from a CT scan. Density segmentation techniques are used to geometrically define the knee bone structure and the encapsulated soft tissues configuration. Linear and non-linear elastic constitutive material models are implemented to mechanically characterize the behaviour of the biological materials. Preliminary numerical results for the model qualitative evaluation are presented.*

**Keywords:** *Finite element, modelling, ACL reconstruction, 3D knee Model, CT scan*

## 1. Introduction

Geometric complexity and non linearity of the materials of the knee make the analytical solutions of the mechanical behaviour of the knee joint difficult. The knee is the most complex joint within the human body. Proper motion of the joint relies significantly on the function of the soft tissue constituents including the four ligaments of the tibiofemoral joint. These ligaments allow primarily flexion/extension and rotation of the joint by enabling the bony constituents (femur and tibia) to translate and rotate relative to each other. In addition to the ligaments, soft cartilage in the joint space permits nearly frictionless contact between the bones.

Computational modeling of the knee provides a way for better understanding the interplay between the hard and soft tissue constituents of the knee during normal and pathologic function (Bischoff et al., 2008). Additionally, properly validated models can be used in the design of knee implant systems by understanding the mechanics of the restored knee and guiding optimization of the design in order to more closely replicate the healthy knee.

This paper presents a numerical method applicable to the bone and soft tissue biomechanics of the ACL reconstructed knee. The paper uses a finite element model to analyse an anatomically detailed three-dimensional ACL reconstructed knee joint using medical image data obtained from a CT scan.

A geometrical model and mesh design for the component parts (pre-processing) were created using the software package program Mimics 10 (Mimics, 2007). The data analysis (post-

processing) and numerical resolutions (solver) were performed with the Abaqus 6.7 (Abaqus, 2007).

The Mimics software is an image-processing package with 3D visualization functions that interfaces with common scanner formats. It is an interactive tool for the visualization and segmentation of CT images as well as MRI images and 3D rendering of objects.

The software enables the user to control and correct the segmentation of CT-scans and MRI-scans. For instance, image artifacts coming from metal implants can be removed. It is also a general-purpose segmentation program for gray value images. It can process any number of 2D image slices (rectangular images are allowed). The interface created to process the images provides several segmentation and visualization tools.

Abaqus is a finite element code that is fully vectorised for use on computers. It uses an interactive post-processing protocol that provides displays and output lists from restart and results files written by the code. A basic concept in the code is the division of the problem history into steps, a step being any convenient phase of the history, such as thermal transient, a creep load, a dynamic transient, etc.

In this code the time incrementation scheme is fully controlled by the stability limit of a central difference operator. The time incrementation is thus fully automatic and requires no user intervention. User-specified time incrementation is not available in the code.

The Abaqus element library enables structures to be modelled using various types of geometrical elements. All elements use numerical integration to allow complete generality in materials behaviour. All of the elements in the code are formulated in a global Cartesian coordinate system except the axisymmetric elements, which are formulated in r-z coordinates. In almost all elements, primary vector quantities (such as displacements and rotation) are defined in terms of nodal values with scalar interpolation functions. Moreover, the Abaqus material library contains a range of linear and non-linear material models for various categories of materials. The mechanical constitutive equations include elastic and inelastic responses.

## **2. FE modelling of a tibial tendon graft ACL reconstruction**

A 3D anatomically detailed model of the ACL reconstructed knee was created using density segmented Computed Tomography (CT) scans (DICOM standard images). This technique geometrically defines the knee bone structure and the encapsulated soft tissues configuration. Linear and nonlinear elastic material models were used to mechanically analyse the behaviour of the biological materials.

The geometrical complexity of the knee structure implies the use of reverse engineering tools e.g. CT scanning, in order to obtain a model that accurately simulates the biomechanical behaviour of the knee, the fixation zone and the ligament (tendon graft).

## 2.1 3D modelling methodology

The complex mechanical behaviour of the knee and the necessity of obtaining accurate results for post validation with experimental values imply an adequate modelling of the knee structure in terms of 3D anthropometrical characteristics and material constitution. The anthropometrical data was obtained from a CT scan of the knee region of a 22 years old male three months after an ACL operation. The DICOM images generated in the CT scan were then processed with the Mimics 10 software to obtain the primary 3D model using density segmentation techniques. The generated primary 3D models were then processed and assembled as geometrical data files. Finally, the model was exported to a FEA package (Abaqus 6.7). The model was then prepared for the analysis by definitions of loads, boundary conditions, material constitutive models, kinematic constraints and mesh discretization processes. The methodology is represented in Fig. 1.

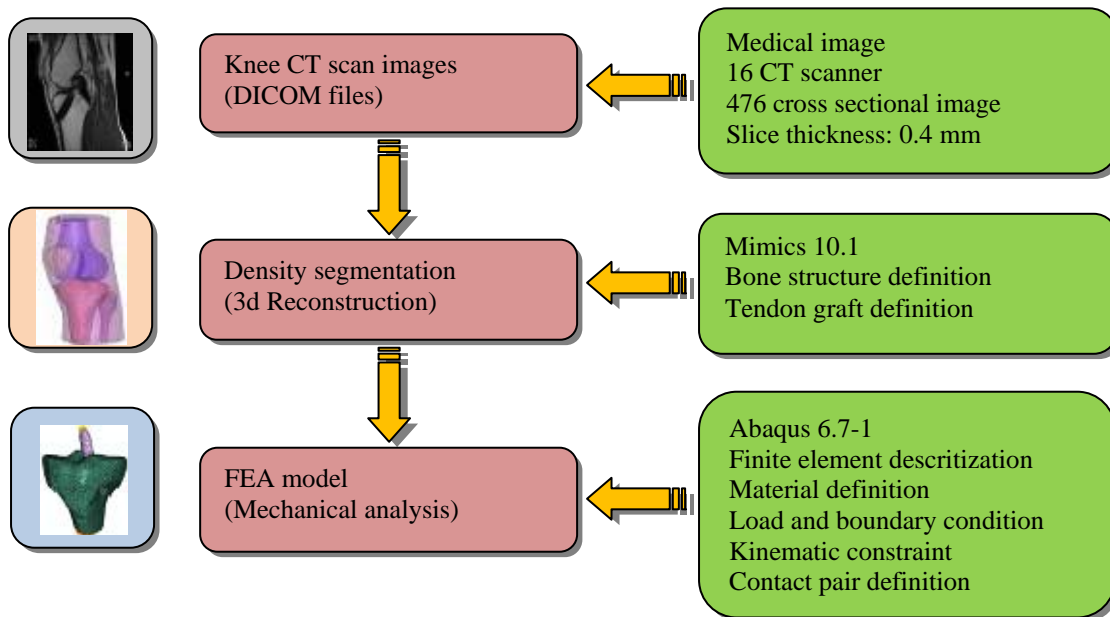


Fig. 1. Modelling methodology of the 3D modelling of an ACL reconstructed knee

## 2.2 Medical image data generation

A CT scan was performed on a 22 years old male using CT equipment (16CT). Scans were performed on the ACL reconstructed knee at the neutral posture where there is the least tension or pressure on tendons, muscles and bones. The scans were made up of 467 cross-sectional “cuts” with a slice distance of 0.4 mm and a field of view (FOV) of 346 mm. The images were exported from the CT equipment in the DICOM format with an image area of 1024x1024 pixels. The high

image resolution associated with the reduced distance between slices assures a good geometrical definition of the primary 3D models in the future density segmentation operations. Fig. 2 shows a single slice of a gray value image (DICOM format) of the reconstructed knee.



Fig. 2. CT scan equipment (right) and a single slice of a gray value image of an ACL reconstructed knee of a 22 years old male using CT scan (left). The scan was obtained 3 months after operation.

### 2.3 Density segmentation (3D reconstruction)

For the reconstruction of the primary 3D anthropometrical models (bone structure and encapsulated soft tissues) the Mimics10.1 medical imaging density segmentation software was used. The DICOM image files generated in the CT scan are constituted by pixels with different gray intensities. The different intensity fields correspond to different material densities in the anatomic knee structure, namely, soft tissues and bone. Note that in a CT scan it is possible to distinguish the tendon graft (ligament) structure. However the positions of the tendon graft and bio-absorbable screw in the tibial tunnel were not clear as the provided CT picture of the knee was three months after the operation. Therefore the tendon graft was reconstructed manually by the software.

The separated 3D reconstruction of each bone segment was accomplished with manual editing operations of the density masks. The reconstruction of the encapsulated soft tissues was faster and easier due to the high difference of densities between the soft tissues and the surrounding air. The spaces between bones normally occupied by cartilages and sinovial liquid were not segmented. The different phases accomplished for the 3D reconstruction using density segmentation techniques with the Mimics10.1 software are presented bellow.

#### 2.3.1 Importing the medical data (DICOM images)

The Mimics software allows automatic importation of the 467 slice images generated in the CT scan. A pixel size of 0.338mm was automatically calculated accounting the present image resolution (1024x1024 pixels) and the acquisition FOV (field of view). The slice distance was correctly determined corresponding to 0.4mm. The pixel size and the slice distance guarantees the coherent dimensional reproducibility of the models generated during the segmentation process. To

minimize the project size and maximize the productivity of the 3D reconstruction process, a crop operation was conducted in order to eliminate the slice images of the left knee, concentrating the modelling efforts in the right knee area.

### **2.3.2 Thresholding**

CT images are a pixel map of the linear X-ray attenuation coefficient of tissue. The pixel values are scaled so that the linear X-ray attenuation coefficient of air equals -1024 and that of water equals 0. This scale is called the Hounsfield (HU) scale (Mimics, 2007).

Thresholding based on Hounsfield scale was used to separate each part of the knee including bones and the encapsulated soft tissues volume. In order to include all the cortical and trabecular bone at the knee bone structure and exclude the cartilage regions, a lower limit of 485HU and an upper limit of 1467HU were defined. The soft tissues region was generated accounting a range of -188HU to 3071HU.

### **2.3.3 Segmentation density masks**

For each bone, individual and separated masks were created. This process allows the posterior generation of independent geometrical files and 3D models. Some manual operations to eliminate residual pixels were conducted. Cavity fill operations to rule out some voids at the density masks were also realized in order to obtain independent and smoother primary 3D models. For a better visualization of the internal boundaries in the density masks, polylines were generated what allows the use of the “Cavity fill from polylines” tool, in order to eliminate in an easier way, mask's internal voids.

### **2.3.4 Region growing**

The region growing process allows splitting the segmentation in different and separated parts, corresponding each part to one mask that can be distinguished by the different applied mask's colours. For that geometrical separation to happen, the adjacent masks must not be connected with any residual pixel. These operations were performed in all slices generated at the CT scan. For the complete definition of the bone knee structure and soft tissues, different regions (tibia, femur, patella, fibula, tendon graft and soft tissue) were defined. Fig. 3 shows the sagittal and coronal views of an region growing process on the ligament.

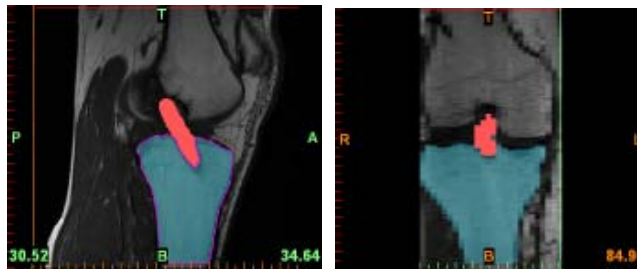


Fig. 3. Region growing process in the sagittal view (left) and coronal view (right) of the ACL reconstructed knee.

### 2.3.5 3D reconstruction

The generated region masks were used to develop 3D models for each the bones and encapsulated soft tissues volume. The 3D reconstruction is based on 3D interpolation techniques that transform the 2D images (slices) in a 3D model. For this reconstruction case, gray values interpolation was used associated with the accuracy algorithm for achieving a more accurate dimensional representation of the knee structure. Shell and triangle reduction, respectively, were used for eliminating small inclusions and reducing the number of mesh elements. Each region was then reconstructed to obtain all the bones and encapsulated soft tissues volume that geometrically defines the knee structure. The relative position of the different parts constituting the primary model assembly of the knee model is shown in Fig. 4.

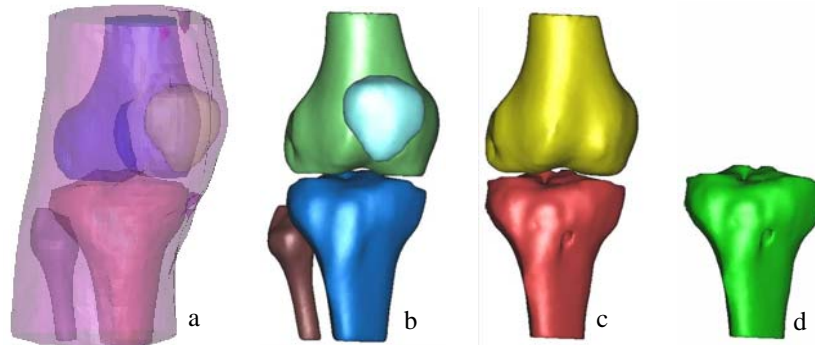


Fig. 4. Encapsulated soft tissue (a); bone structure assembly (b); tibia and femur (c); tibia bone (d)

However, only tibial bone and tendon graft (Fig. 5) files were generated in Mimics software and considered for further process in this study. The files generated in Mimics software were then assembled together. A volume boolean operations were performed to achieve a volume of soft

tissues that corresponds to the bone structure coupled with the tendon graft. This approach guarantees the perfect alignment of the models exterior surfaces, what is very important to the future finite element model generation.

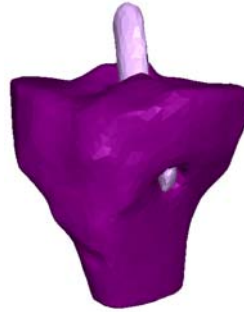


Fig. 5. 3D model of the tibial bone with a reconstructed tendon graft generated by the Mimics software

## 2.4 Mesh definition

The finished 3D model in surface mesh format was imported in the FEA package Abaqus 6.7. The surface mesh “tri” (triangular element type) was converted to a volume mesh “tet” (tetrahedral element type) by the software. The model consisted of the tibial bone and tendon graft. Fig. 6 shows the finite element model of the tibial bone and tendon graft.

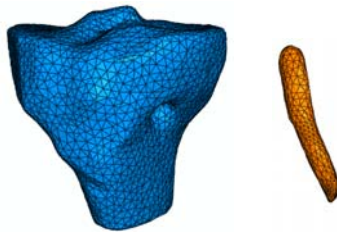


Fig. 6. FE model of the tibial bone and tendon graft. The mesh was converted from triangular surface element type to a tetrahedral volume element type.

The assembly of tibial bone and tendon graft is presented in Fig. 7. The bone was bonded to the tendon graft volume using mesh tie kinematic constraints.

The tendon graft was geometrically simplified in the 3D model and a variety of 3D element topology was used to discretize the model structure. However, the tibial bone and graft geometrical complexity do not allow the use of hexahedral elements which usually provide higher accuracy with less computational cost. For this reason, tetrahedral elements that are more able to capture the irregularly shapes of the tibial bone and tendon graft, were used to mesh the model. This type of element is able to withstand large deformation.

The bone and tendon graft were modelled using a large number of linear tetrahedral elements (C3D4), each with six degrees of freedom per node. Total numbers of node for the tendon graft and tibial bone were 587 and 8117 respectively but Total elements number of the tendon graft and tibial bone were 2179 and 41516 respectively.

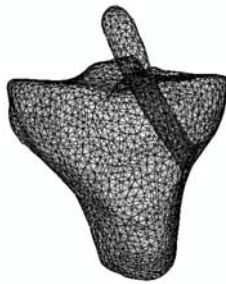


Fig. 7. Assembly of a 3D mesh model of the tibial bone and tendon graft in a transparency view.

## 2.5 Contact algorithm and boundary condition

Different contact algorithms are available in Abaqus code. The contact constraints are applied in a discrete manner, meaning that a node on one surface is constrained (the slave surface) not to penetrate the other surface (the master surface). The nodes on the master surface can however in principle, penetrate the slave contact boundary unhindered.

For each increment of the analysis, Abaqus advances the kinematic state of the model into a predicted configuration without considering the contact condition. Then it determines which slave nodes in the predicted configuration penetrate the master surfaces. The depth of each slave node's penetration, the mass associated with it and the time increment are used to calculate the resisting force required to prevent penetration. This is the force which, had it been applied during the increment, would have caused the slave node to exactly contact the master surface. When the master surface is formed by element faces the resisting forces of all the slave nodes are distributed to the nodes on the master surface.

Penalty and Kinematic contact algorithms are available in the code. The penalty contact algorithm results in less stringent enforcement of contact constraints than the kinematic contact algorithm, but the penalty algorithm allows for the treatment of more general types of contact (for example,

contact between two rigid bodies). When the penalty method is chosen for enforcing contact constraints in the normal direction, it is also used to enforce sticking friction.

The penalty contact algorithm searches for slave node penetrations. Contact forces proportional to the penetration distance are applied to the slave nodes to oppose the penetration, while equal and opposite forces act on the master surface at the penetration point. When the master surface is formed by element faces, contact forces are distributed to nodes of the master faces being penetrated.

The boundary condition was defined to allow the load transmission between the tibial bone and tendon graft. The surfaces interaction definition allows the generation of a contact pressure field at the tunnel area. A small sliding tracking approach associated with a node to surface contact formulation was defined to model the interaction tangential behaviour. The friction coefficient between the bone tunnel and tendon graft was set to 0.25 (Chizari et al, 2007), using the penalty friction method.

A pure tensile load of 200N directed along the tunnel axis toward the femur which approximates the graft tension at full extension of the knee during gait (Harrington et al, 1976), was applied to the tendon graft.

A tied interaction was defined between the bone tunnel and tendon graft corresponding to the length of the fixation (30 mm). The bottom side boundary of the tibial bone was fixed in X,Y,Z directions.

The velocity field, which is part of the algorithm used in the explicit finite element code, was assumed to be linear and continuous at the interface between the tunnel and tendon graft to enable the deformation to be modelled as a function of time.

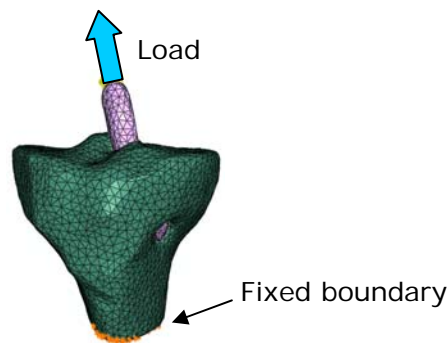


Fig. 8. Load and boundary condition in the FE model. The graft was loaded along the tunnel axis and the tail end of the tibial bone was fixed in X,Y,Z directions.

## 2.6 Material properties

Material properties which determine the relationship between the stresses and strains had to be derived for the bone and soft tissue. While the mechanical properties of the individual organelles of a bone and tendon graft are difficult to determine, the model referred in this study will allow at least a partial determination of the simplified material properties.

The study assumes a linear elastic behaviour for the bone and tendon graft, which is adequate for the study of stress and strain (Cowin et al, 1989). An isotropic Poisson's ratio was used (Williams et al, 1982) in the model for the bone and tendon graft. The shear modulus for bone can be calculated from empirical relationships reported by Ashman et al. (1989). The bone was assumed as isotropic (Choi et al, 1990, Brown et al, 1984) and homogeneous. The general material properties are listed in Table 1.

Table 1. Material property of bone, ACL ligament and tendon (Standard Handbook, 2003).

	Cortical Bone	Cancellous bone	ACL Ligament	Tendon
Density, g/cm <sup>3</sup>	2.21	1.15	1.2	1.95
Young's modulus, MPa	13400	283	303	1604
Poisson's ratio	0.24	0.29	0.28	0.27

## 3. Preliminary results

The created FE model allows the output of several results that can be used for evaluating of the tibial tendon graft fixation. The monitoring of stress values in the tunnel area assumes a vital role in this study. The following results were obtained considering pure tensile load on the tendon graft.

The maximum stress was monitored in the distal end of the tibial tunnel where the tendon leaves the fixation. The pattern of Mises stress in the different sections of the tunnel is shown in Fig. 9. The model predicts a maximum stress value of 0.199 MPa on the tendon graft in the tibial tunnel at the fixation zone. It should be noted that the fixation device has been ignored in the model as a bio-absorbable screw was used for the fixation and it was assumed that the screw had been absorbed to the body.

The pattern of the stress on the cortical bone during the tensile loading of the graft is shown in Fig. 10. The results show that the level of stress on the cortical bone is lower than that on the cancellous bone. It means we can apply more stress on the cortical bone and improve the strength of the fixation if the fixation is in contact with the cortical bone.

The cross-sectional pattern of stress in the region of fixation is shown in Fig. 11. The distal end of the tunnel shows the widest stress pattern and higher levels of stress. The radial distribution of the stress is likely to depend on the section viewed and may not be the same in different sections, especially where the section is close to the distal end of the tunnel.

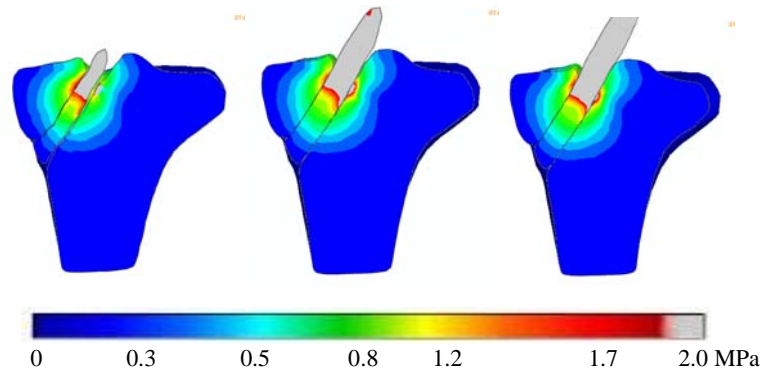


Fig. 9. Longitude sections of the tibial tunnel. The contour shows the level of Mises stress on the bone and tendon graft.

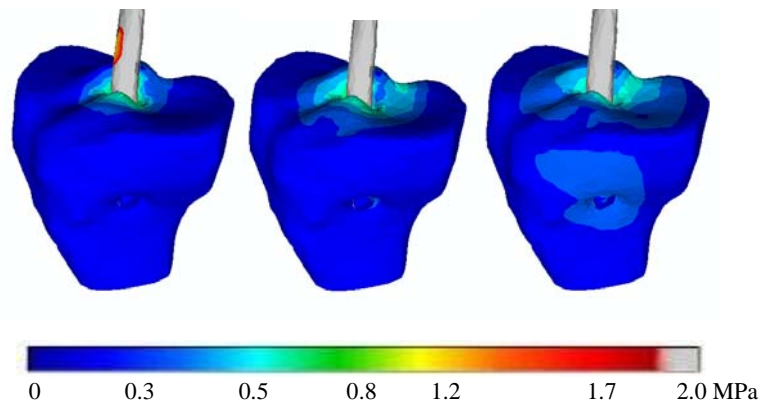
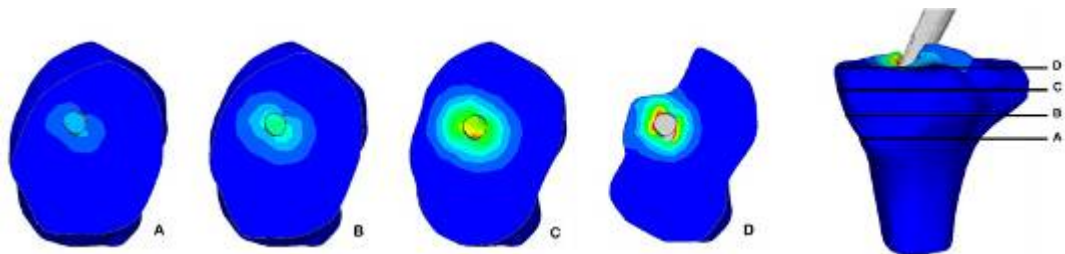


Fig. 10. Three stages of the reconstructed tibial bone during the tensile loading on the tendon graft



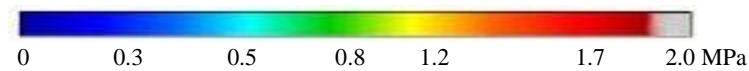


Fig. 11. Different sections of the tibial bone and tunnel zone during the tensile loading on the tendon graft. The contour shows level of Mises stress on the bone and tendon graft

#### 4. Conclusions

This study presents a numerical method applicable to the bone and tendon graft biomechanics of an ACL repaired knee after. The study uses a finite element method to analyse an anatomically detailed ACL reconstructed knee of a 22 years old patient three months after operation, using data obtained from a CT scan. The model considered a kinematic constraint and parts interaction at the tendon graft and tibial tunnel were implemented. The monitoring of mechanical parameter such as stress at the tunnel and ligament was the main objective and was achieved by geometrical simplifications of the tendon graft.

The maximum stress monitored in the distal end of the tibial tunnel where the tendon leaves the fixation. A maximum stress value of 0.199 MPa was predicted on the tendon graft in the tibial tunnel at the fixation zone. Although the results show that the level of stress on the cortical bone is lower than that on the cancellous bone. The current numerical modelling is assumed the bone and tendon graft are linear elastic, isotropic and homogeneous. Further non-linear analyses and failure mechanisms are needed to achieve a complete understanding on the sutured tendon response under tensile loading

#### 5. References

1. Abaqus, User's Manual, Version 6.7, HKS Inc., Providence, Rhode Island, 2007.
2. Ashman R.B., Rho J.Y., Turner C.H., "Anatomical variation of orthotropic elastic moduli of the proximal human tibia". *Journal of Biomechanics*. 22, 895-900, 1989.
3. Chizari M., Wang B. and Snow M., "Experimental and numerical analysis of screw fixation in anterior cruciate ligament reconstruction", *World Congress on Engineering 2007 (ICSBB'07)*, 1439-1442, 2007.
4. Choi K., Kuhn J.L., Ciarelli M.J., Goldstein S.A., "The elastic moduli of human subchondral, trabecular, and cortical bone tissue and the size-dependency of cortical bone modulus". *Journal of Biomechanics* 23, 1103-1113, 1990.
5. Cowin S.C. (Ed.), "Bone Mechanics". CRC Press, Boca Raton, FL.
6. Brown T.D., A.M. DiGioia, "A contact-coupled finite element analysis of the natural adult hip". *Journal of Biomechanics* 17, 437-448, 1989.

7. Bischoff J.E., Siggelkow E., Sieber D., Kersh M., Ploeg H., Münchinger M., “Advanced Material Modeling in a Virtual Biomechanical Knee”, Abaqus Users’ Conference, 2008
8. Harrington I.J., “A bioengineering analysis of force actions at the knee in normal and pathological gait”. Biomedical Engineering 11, 167-172, 1976.
9. Mimics, Reference Guide, Version 10.1, Materialise N.V., 2007.
10. Standard Handbook of Biomedical Engineering & Design, Myer Kutz, Ed., McGraw-Hill, New York, 2003.
11. Williams J.L., Lewis J.L., “Properties and an anisotropic model of cancellous bone from the proximal tibial epiphysis”. Transactions of ASME, Journal of Biomechanical Engineering 104, 50-56, 1982.